Sidelobe Suppression for Robust Capon Beamforming With Mainlobe-to-Sidelobe Power Ratio Maximization

Yipeng Liu and Qun Wan, *Member, IEEE*

***Abstract*—High sidelobe level is a major disadvantage of the Capon beamforming. To suppress the sidelobe for interference nulling, this letter introduces a mainlobe-to-sidelobe power ratio maximization constraint to the Capon beamforming. Its relaxed convex programming model minimizes the sidelobe power while keeping the mainlobe power constant. Simulations show that the obtained beamformer outperforms the Capon beamformer and sparse Capon beamformer.**

***Index Terms*—Array signal processing, robust Capon beamforming, sidelobe suppression.**

I. Introduction

A BEAMFORMER is a multiple-antennas system that makes spatial beam focused on the target direction and spatial beam nulled interference signal. In this system, each transmit antenna is weighted by a properly designed gain and phase shift before transmission. It is used extensively to improve the performance in a variety of areas such as radar, sonar, and wireless communications [1].

The Capon beamformer is one of the most popular beamforming systems. It is a data-dependent beamformer that minimizes the array output power subject to the linear constraint that the signal-of-interest (SOI) does not suffer from any distortion by adaptive selection of the weight vector. The Capon beamformer has better resolution and much better interference rejection capability than the data-independent beamformer. However, its high sidelobe level and the SOI steering vector uncertainty due to differences between the assumed signal arrival angle and the true arrival angle would seriously degenerate the performance in the presence of environment noise and interferences [1]–[3].

With a spherical uncertainty set introduced, doubly constrained robust (DCR) Capon beamformer is obtained with the increased robustness against direction-of-arrival (DOA) mismatch [5]. To achieve a faster convergence speed and a higher steady-state signal-to-interference-plus-noise ratio (SINR), [6] constrains its weight vector to a specific conjugate symmetric form. In [7], by iterative estimation of the actual steering vector based on conventional robust Capon beamforming (RCB) formulation, iterative robust Capon beamformer (IRCB) with adaptive uncertainty level is proposed to enhance the robustness against DOA mismatch. Many works have been done to enhance the robustness against the SOI steering vector uncertainty, to accelerate the convergence, etc. [8].

Recently, a sparse constraint in the form of the L1 norm is put onto the interference and background noise [4]. Similarly, based on the Capon criterion, a new constraint is added to maximize the mainlobe-to-sidelobe power ratio (MSPR) to shape the beam pattern here. As more power is accumulated in the mainlobe area, the robustness against SOI steering vector uncertainty is improved; as less power is in the sidelobe area, the interference and noise rejection capability can be enhanced. Therefore, a better performance can be achieved. Numerical results also demonstrate the performance of the proposed beamformer.

II. Signal Model

The signal impinging into a uniform linear array (ULA) with M antennas can be represented by an M-by-1 vector [1]

$$\mathbf{x}(k) = s(k)\mathbf{a}(\theta_0) + \sum_{j=1}^{J} \beta_j(k)\mathbf{a}(\theta_j) + \mathbf{n}(k) \tag{1}$$

where k is the index of time; J is the number of interference sources; $s(k)$ and $j(k)$ (for $j = 1, \ldots, J$) are the amplitudes of the SOI and interfering signals at time instant k, respectively;θ_l (for $l = 0, 1, \ldots, J$) are the DOAs of the SOI and interfering signals; $\mathbf{a}(\theta_l) = [1 \quad \exp(j\varphi_l) \quad \cdots \quad \exp(j(M-1)\varphi_l)]^T$ (for $l = 0, 1, \ldots, J$) are the steering vectors of the SOI and interfering signals, wherein $\varphi_l = (2\pi d/\lambda)\sin\theta_l$, with d being the distance between two adjacent sensors and λ being the wavelength of the SOI; and $\mathbf{n}(k)$ is the additive white Gaussian noise (AWGN) vector at time instant k.

The output of a beamformer for the time instant k is then given by

$$\begin{aligned} y(k) &= \mathbf{w}^H\mathbf{x}(k) \\ &= s(k)\mathbf{w}^H\mathbf{a}(\theta_0) + \sum_{j=1}^{J} \beta_j(k)\mathbf{w}^H\mathbf{a}(\theta_j) + \mathbf{w}^H\mathbf{n}(k) \end{aligned} \tag{2}$$

Manuscript received May 15, 2012; revised July 18, 2012 and September 13, 2012; accepted October 03, 2012. Date of publication October 09, 2012; date of current version October 26, 2012. This work was supported in part by the FWO of Flemish Government under Grant G.0108.11 (Compressed Sensing) and the National Natural Science Foundation of China under Grant 61172140. *(Corresponding author: Q. Wan.)*

Y. Liu is with the Electronic Engineering Department, University of Electronic Science and Technology of China (UESTC), Chengdu 611731, China, and also with the Department of Electrical Engineering, ESAT-SCD/IBBT Future Health Department, KU Leuven, 3001 Heverlee, Belgium (e-mail: yipeng.liu@esat.kuleuven.be).

Q. Wan is with the Electronic Engineering Department, University of Electronic Science and Technology of China (UESTC), Chengdu 611731, China (e-mail: wanqun@uestc.edu.cn).

Color versions of one or more of the figures in this letter are available online at http://ieeexplore.ieee.org.

Digital Object Identifier 10.1109/LAWP.2012.2223451

where $\boldsymbol{w}$ is the M-by-1complex-valued weighting vector of the beamformer.

III. Proposed Beamformer

The Capon beamformer is defined as the solution to the following linearly constrained minimization problem [1]:

$$\mathbf{w}_{\text{Capon}} = \arg\min_{\mathbf{w}}(\mathbf{w}^H\mathbf{R}_x\mathbf{w}),\ \text{s. t. } \mathbf{w}^H\mathbf{a}(\theta_0) = 1 \tag{3}$$

where $\mathbf{R}_x$ is the M-by-M covariance matrix of the received signal vector $\mathbf{x}(k)$, and $\mathbf{w}^H\mathbf{a}(\theta_0) = 1$ is the distortionless constraint applied on the SOI.

To suppress the sidelobe, a sparse constraint for the beam pattern is incorporated in the Capon beamformer (3)

$$\mathbf{w}_S = \arg\min_{\mathbf{w}}(\mathbf{w}^H\mathbf{R}_x\mathbf{w} + \gamma_1\|\mathbf{w}^H\mathbf{A}\|_1),\quad \text{s. t. } \mathbf{w}^H\mathbf{a}(\theta_0) = 1 \tag{4}$$

where γ_1 is the weighting factor balancing the minimum variance constraint and the L1 norm minimization constraint. The M-by-N $\mathbf{A}$ is the array manifold with αn's $(n = 1, 2, \ldots, N)$ being the sampled angles in the $[-90°, 90°]$, and the N steering vectors cover all the DOAs in the sampling range, with α_0 being the DOA of the SOI as defined in (1), i.e.,

$$A_{mn} = \exp(j(m-1)\varphi_n),\quad \text{for } m = 1, \ldots, M;\ n = 1, \ldots, N \tag{5}$$

$$\varphi_n = \frac{2\pi d}{\lambda}\sin\alpha_n,\quad \text{for}\quad n = 1, \ldots, N. \tag{6}$$

In the perspective of the beam pattern, it is observed from the Capon beamformer (3) that there is only an explicit constraint on the desired DOA, i.e., $\mathbf{w}^H\mathbf{a}(\theta_0) = 1$, while no constraint is put onto the interference and background noise. To repair this drawback, we propose the following cost function with a regularization term, which forces maximization of the MSPR:

$$\mathbf{w}_{\text{MSPR}} = \arg\min_{\mathbf{w}}\left\{\mathbf{w}^H\mathbf{R}_x\mathbf{w} + \gamma_2\frac{\|\mathbf{w}^H\mathbf{A}_S\|_2^2}{\|\mathbf{w}^H\mathbf{A}_M\|_2^2}\right\}\quad \text{s. t. } \mathbf{w}^H\mathbf{a}(\theta_0) = 1 \tag{7}$$

where γ_2 is the weighting factor balancing the minimum variance constraint and the MSPR maximization constraint

$$\mathbf{A}_M = [\,\mathbf{a}(\theta_{-b})\ \cdots\ \mathbf{a}(\theta_0)\ \cdots\ \mathbf{a}(\theta_{+b})\,] \tag{8}$$

$$\mathbf{A}_S = [\,\mathbf{a}(\theta_{-90})\ \cdots\ \mathbf{a}(\theta_{-b-1})\ \ \mathbf{a}(\theta_{+b+1})\ \cdots\ \mathbf{a}(\theta_{+90})\,]. \tag{9}$$

$\mathbf{A}_S$ is submatrix of the steering matrix $\mathbf{A}$, and it is constituted with the sidelobe steering vectors in $\mathbf{A}$. $\mathbf{A}_M$ is submatrix of the steering matrix $\mathbf{A}$ as well, and it is constituted with the mainlobe steering vectors in $\mathbf{A}$. b is an integer corresponding to the bounds between the mainlobe and the sidelobe of the beam pattern.

Physically $\mathbf{w}^H\mathbf{a}(\theta)$ is the array gain in the signal direction θ. The product $\mathbf{w}^H\mathbf{A}_S$ indicates array gains of the sidelobe; and the product $\mathbf{w}^H\mathbf{A}_M$ indicates array gains of the mainlobe. With the term $\|\mathbf{w}^H\mathbf{A}_S\|_2^2/\|\mathbf{w}^H\mathbf{A}_M\|_2^2$ minimized, the MSPR-Capon beamformer (7) can perform sidelobe minimization and mainlobe maximization simultaneously. However, unfortunately it is not convex. To convexity it, we relax the MSPR constraint and obtain a new beamformer as

$$\mathbf{w}_{\text{RMSPR}} = \arg\min_{\mathbf{w}}\left\{\mathbf{w}^H\mathbf{R}_x\mathbf{w} + \gamma_3\left[\left(\|\mathbf{w}^H\mathbf{A}_M\|_2^2 - 1\right)^2 + \|\mathbf{w}^H\mathbf{A}_S\|_2^2\right]\right\}\quad \text{s. t. } \mathbf{w}^H\mathbf{a}(\theta_0) = 1 \tag{10}$$

where γ_3 is the weighting factor balancing the minimum variance constraint and the relaxed MSPR (RMSPR) maximization constraint.

The splitting of the matrix $\mathbf{A}$ into $\mathbf{A}_M$ and $\mathbf{A}_S$ helps. The newly added RMSPR term $(\|\mathbf{w}^H\mathbf{A}_M\|_2^2 - 1)^2 + \|\mathbf{w}^H\mathbf{A}_S\|_2^2$ is convex. It is minimized to minimize the sidelobe power $\|\mathbf{w}^H\mathbf{A}_S\|_2^2$ and the approximation error $(\|\mathbf{w}^H\mathbf{A}_M\|_2^2 - 1)^2$. It is one kind of way to reshaping the Capon beam pattern with constraint on both mainlobe and sidelobe. The mainlobe power and sidelobe power are constrained separately in the optimization model (10). It is no doubt that the minimization of $\|\mathbf{w}^H\mathbf{A}_S\|_2^2$ gives smaller power of sidelobe. The minimization $(\|\mathbf{w}^H\mathbf{A}_M\|_2^2 - 1)^2 \le \varepsilon$ makes the power of mainlobe be a constant approximately. i.e., for $(\|\mathbf{w}^H\mathbf{A}_M\|_2^2 - 1)^2 \le \varepsilon$, if ε is very small, the power of mainlobe can be approximately constant. Specially, if $\varepsilon = 0$, the mainlobe power is strictly constant. Combining these two constraints for beam pattern, it forces the power of mainlobe $\|\mathbf{w}^H\mathbf{A}_M\|_2^2$ to be approximately constant while making the power in sidelobe $\|\mathbf{w}^H\mathbf{A}_S\|_2^2$ as small as possible. With the power in mainlobe being an approximate constant and the power in sidelobe being minimized, the MSPR can be maximized in a relaxed way. Thus, the relaxed form of the maximization of MSPR $\|\mathbf{w}^H\mathbf{A}_M\|_2^2/\|\mathbf{w}^H\mathbf{A}_S\|_2^2$ would be achieved.

The proposed optimization model (10) is a second-order cone programming (SOCP) and can be solved by convex optimization software [9]. An iterative way can be obtained by the Lagrange multiplier methods as well. Here, we use γ instead of γ_3. First, the Lagrange multipliers technique is used to combine the constraints in (7) into the objective function

$$\begin{aligned} f(\mathbf{w}) &= \mathbf{w}^H\mathbf{R}_x\mathbf{w} + \gamma\left(\|\mathbf{w}^H\mathbf{A}_M\|_2^2 - 1\right)^2 \\ &\quad + \gamma\|\mathbf{w}^H\mathbf{A}_S\|_2^2 + \mu(\mathbf{w}^H\mathbf{a}(\theta_0) - 1) \\ &= \mathbf{w}^H\mathbf{R}_x\mathbf{w} + \gamma\left(\mathbf{w}^H\mathbf{A}_M\mathbf{A}_M^H\mathbf{w} - 1\right)^2 \\ &\quad + \gamma\mathbf{w}^H\mathbf{A}_S\mathbf{A}_S^H\mathbf{w} + \mu(\mathbf{w}^H\mathbf{a}(\theta_0) - 1). \end{aligned} \tag{11}$$

Thus, we have

$$\frac{\partial f(\mathbf{w},\mu)}{\partial\mathbf{w}^H} = \mathbf{R}_x\mathbf{w} + \gamma\left(\mathbf{w}^H\mathbf{A}_M\mathbf{A}_M^H\mathbf{w} - 1\right)\left(2\mathbf{A}_M\mathbf{A}_M^H\mathbf{w}\right) + \gamma\mathbf{A}_S\mathbf{A}_S^H\mathbf{w} + \mu\mathbf{a}(\theta_0) \tag{12}$$

$$\frac{\partial f(\mathbf{w},\mu)}{\partial\mu} = 0 \Rightarrow \mathbf{w}^H\mathbf{a}(\theta_0) = 1. \tag{13}$$

From (12)

$$\left(\mathbf{R}_x + \gamma\left(2\mathbf{w}^H\mathbf{A}_M\mathbf{A}_M^H\mathbf{w} - 2\right)\mathbf{A}_M\mathbf{A}_M^H + \gamma\mathbf{A}_s\mathbf{A}_S^H\right)\mathbf{w} = -\mu\mathbf{a}(\theta_0) \tag{14}$$

$$\mathbf{w} = -\mu\left(\mathbf{R}_x + \gamma\left(2\mathbf{w}^H\mathbf{A}_M\mathbf{A}_M^H\mathbf{w} - 2\right) \times \mathbf{A}_M\mathbf{A}_M^H + \gamma\mathbf{A}_s\mathbf{A}_S^H\right)^{-1}\mathbf{a}(\theta_0)0 \tag{15}$$

Substituting (15) into (13) gives

$$-\mu \mathbf{a}(\theta_0)^H \mathbf{\Xi} \mathbf{a}(\theta_0) = 1 \tag{16}$$

where

$$\mathbf{\Xi} = \left(\left(\mathbf{R}_x + \gamma \left(2\mathbf{w}^H \mathbf{A}_M \mathbf{A}_M^H \mathbf{w} - 2 \right) \mathbf{A}_M \mathbf{A}_M^H + \gamma \mathbf{A}_s \mathbf{A}_S^H \right)^H \right)^{-1}. \tag{17}$$

Then

$$\mu = \frac{-1}{\mathbf{a}(\theta_0)^H \mathbf{\Xi} \mathbf{a}(\theta_0)}. \tag{18}$$

Substituting (18) into (15) gives

$$\mathbf{w} = \frac{\mathbf{\Xi} \mathbf{a}(\theta_0)}{\mathbf{a}(\theta_0)^H \mathbf{\Xi} \mathbf{a}(\theta_0)}. \tag{19}$$

Therefore, the iterative algorithm is (20), shown at the bottom of the page, where i denotes the interaction index.

IV. Simulation

In the simulations, a ULA with eight half-wavelength-spaced antennas is considered. The AWGN at each sensor is assumed spatially uncorrelated. The DOA of the SOI is set to be 0°, and the DOAs of three interfering signals are set to be −30°, 30°, and 70°, respectively. The SNR is set to be 10 dB, and the interference-to-noise ratios (INRs) are assumed to be 20, 20, and 40 B in −30°, 30°, and 70°, respectively. One hundred snapshots are used for each simulation. Without loss of generality, b is set to be 12, and γ_1 and γ_3 are chosen to be 5.1 in the first simulation and 9.7 in the second simulation. The matrix $\mathbf{A}$ consists of all steering vectors in the DOA range of $[-90°, 90°]$ with the sampling interval of 1°. The software CVX is used to give the optimal values [9].

To examine its influence on the performance, the SINR is calculated via the following formula:

$$\text{SINR} = \frac{\sigma_s^2 \mathbf{w}^H \mathbf{a}(\theta_0) \mathbf{a}^H(\theta_0) \mathbf{w}}{\mathbf{w}^H \left(\sum_{j=1}^{J} \sigma_j^2 \mathbf{a}(\theta_j) \mathbf{a}^H(\theta_j) + \mathbf{Q} \right) \mathbf{w}} \tag{21}$$

where σ_s^2 and σ_j^2 are the variances of the SOI and jth interference, $\mathbf{Q}$ is a diagonal matrix with the diagonal elements being the noise's variances.

Fig. 1 shows beam patterns of the Capon beamformer (3), the sparse Capon beamformer (4), and the RMSPR-Capon beamformer (10) of 1000 Monte Carlo simulations. The beam pattern of the RMSPR-Capon beamformer has lower array gain level in sidelobe than standard Capon beamformer. However, the sparse Capon beamfomer achieves the lowest array gain in most DOAs in the sidelobe, but its nulls for interference are not accurate. The RMSPR-Capon beamformer provides the deepest nulls in the directions of interferences, i.e., −30°, 30°, and 70°, respectively. The average received SINR by the Capon beamformer, the sparse Capon beamformer (4) and the RMSPR-Capon beamformer (10) are 2.3027, 4.3178, and 6.5224 dB. The RMSPR-Capon beamformer (10) can obtain the best SINR performance. Moreover, when we change the parameters, in 1000 Monte Carlo simulations, the influence of choice of the parameters γ_1 and γ_3 on the output SINR of the RMSPR-Capon beamformer is slight, and almost all the values of SINR lie between 6.4287 and 6.7861 dB.

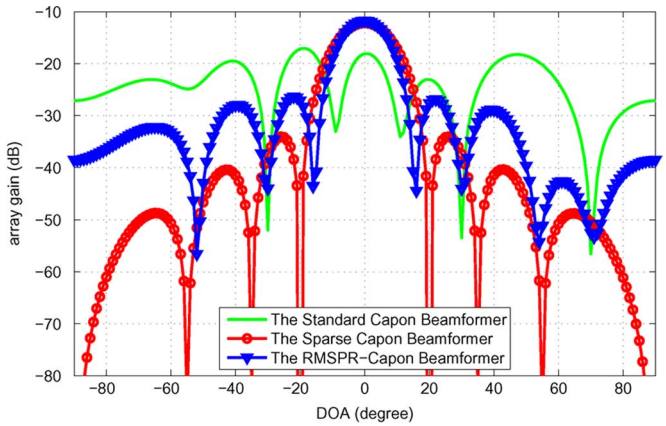

Fig. 1. Normalized beam patterns of the Capon beamformer and the RMSPR-Capon beamformer without mismatch between the steering angle and the DOA of the SOI.

Fig. 2 shows beam patterns of the beamformers that we have discussed, with each beamformer having a 3° mismatch between the steering angle and the DOA of the SOI. We can see that the Capon beamformer has a deep notch in 3°, which is the DOA of the SOI. It can be explained by using the fact that the Capon beamformer is designed to minimize the total array output energy subject to a distortionless constraint in the DOA of the SOI, so when the steering angle is in 3°, instead of 0°, the Capon beam pattern maintains distortionless in 0° while resulting in a deep null in 3°. This observation shows the high sensitivity of the Capon beamformer to steering angle mismatch. Comparing beam patterns of beamformers defined in (3), (4), and (10), we can see that the sparse Capon beamformer and the RMSPR-Capon beamformer have almost the same array gains in the DOA of the SOI. Both of them have lower sidelobe levels and deeper nulls for interference avoidance than the standard Capon beamformer. It is the same as Fig. 1 that although the sparse Capon beamfomer achieves the lower array gain in the sidelobe, its nulls for interference are not accurate.

$$\mathbf{w}(i+1) = \frac{\left(\mathbf{R}_x + \gamma \left(2\mathbf{w}(i)^H \mathbf{A}_M \mathbf{A}_M^H \mathbf{w}(i) - 2 \right) \mathbf{A}_M \mathbf{A}_M^H + \gamma \mathbf{A}_s \mathbf{A}_S^H \right)^{-1} \mathbf{a}(\theta_0)}{\mathbf{a}(\theta_0)^H \left(\left(\mathbf{R}_x + \gamma \left(2\mathbf{w}(i)^H \mathbf{A}_M \mathbf{A}_M^H \mathbf{w}(i) - 2 \right) \mathbf{A}_M \mathbf{A}_M^H + \gamma \mathbf{A}_s \mathbf{A}_S^H \right)^H \right)^{-1} \mathbf{a}(\theta_0)} \tag{20}$$

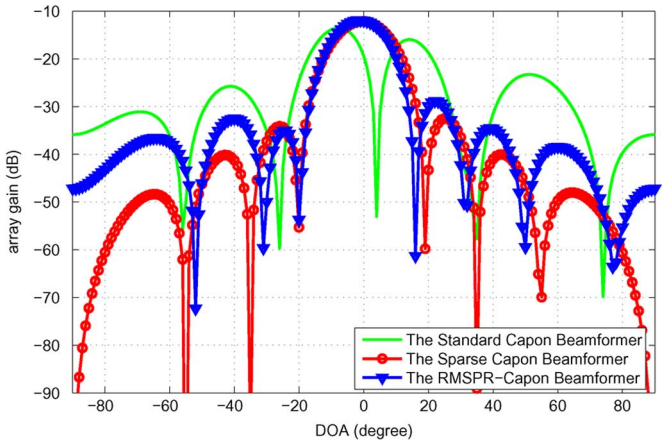

Fig. 2. Normalized beam patterns of the Capon beamformer and the RMSPR-Capon beamformer, with 3° mismatch between the steering angle and the DOA of the SOI.

The RMSPR-Capon beamformer provides the deepest nulls in the all directions of interferences. In the case of 3° mismatch, the average received SINRs by the Capon beamformer (3), the sparse Capon beamformer (4), and the RMSPR-Capon beamformer (10) are 0.0003, 3.1903, and 3.8402 dB, respectively. One thousand Monte Carlo simulations show that the influence of choice of the parameters γ_1 and γ_3 on the output SINR is slight as well, and all the values of SINR lie between 3.6571 and 3.9380 dB for the RMSPR-Capon beamformer.

In the sparse Capon beamformer, the used constraint $\|\mathbf{w}^H\mathbf{A}\|_1$ for reshaping the beam pattern is encouraging sparse distribution in the array gain distribution. It encourages a smaller number of array gains with large amplitudes, no matter the large ones in the mainlobe or sidelobe, because the sparse constraint is combined with other constraints, such as $\min_{\mathbf{w}} \mathbf{w}^H\mathbf{R}_x\mathbf{w}$ and $\mathbf{w}^H\mathbf{a}(\theta_0) = 1$. Most of the larger array gains are in mainlobe. However, a small number of the larger array gains can appear in sidelobe, which can influence the inaccurate nulling. Yet, here the constraint $[(\|\mathbf{w}^H\mathbf{A}_M\|_2^2 - 1)^2 + \|\mathbf{w}^H\mathbf{A}_S\|_2^2]$ is about the total power in mainlobe and sidelobe. It makes the array gains power in mainlobe as larger as possible than the array gains power in sidelobe, which is another way to approximately achieve our goal to get larger array gains in mainlobe and smaller array gains in sidelobe. It is different from sparse constraint $\|\mathbf{w}^H\mathbf{A}\|_1$. Here, we can regard both the sparse Capon beamformer (4) and the RMSPR-Capon beamformer (10) are different "relaxed" ways to the strict MSPR-Capon beamformer (7). Comparing (4) and (10), the latter one may be more suitable for reshaping the Capon beam pattern. That may be why sparse Capon beamformer has some lower array gains in the sidelobe range, but its nulls for interference suppression are not accurate. The newly added constraint of RMSPR-Capon (10) on conventional Capon beamformer does not degenerate the nulling performance, while the newly added sparse constraint of (7) on conventional Capon beamformer does. That is why the final SINR of the RMSPR-Capon (10) is the best.

V. Conclusion

The proposed beamformer introduces a new beam-pattern shaping constraint. it shows superiority to the sparse Capon beamformer. The problems of the Capon beamformer's high sidelobe level as well as sensitivity to SOI steering vector errors are much alleviated. In the future work, the RMSPR constraint can be incorporated to other Capon-based beamformers, such as the DCR Capon beamformer, to further enhance the performance.

References

[1] J. Li and P. Stoica, *Robust Adaptive Beamforming*. New York: Wiley, 2006.
[2] M. Wax and Y. Anu, "Performance analysis of the minimum variance beamformer," *IEEE Trans. Signal Process.*, vol. 44, no. 4, pp. 928–937, Apr. 1996.
[3] H. Cox, "Resolving power and sensitivity to mismatch of optimum array processors," *J. Acoust. Soc. Amer.*, vol. 54, no. 3, pp. 771–785, Sep. 1973.
[4] Y. Zhang, B. P. Ng, and Q. Wan, "Sidelobe suppression for adaptive beamforming with sparse constraint on beam pattern," *Electron. Lett.*, vol. 44, no. 10, pp. 615–616, May 2008.
[5] J. Li, P. Stoica, and Z. Wang, "Doubly constrained robust capon beamformer," *IEEE Trans. Signal Process.*, vol. 52, no. 9, pp. 2407–2423, Sep. 2004.
[6] L. Zhang, W. Liu, and R. J. Langley, "A minimum variance beamformer with linear and quadratic constraints based on uniform linear antenna arrays," in *Proc. LAPC*, Loughborough, U.K., Nov. 16–17, 2009, pp. 585–588.
[7] J. P. Lie, X. H. Li, W. Ser, C. S. See, and L. Lei, "Adaptive uncertainty based iterative robust capon beamformer," in *Proc. IEEE ICASSP*, Dallas, TX, Mar. 14–19, 2010, pp. 2526–2529.
[8] L. Du, T. Yardibi, J. Li, and P. Stoica, "Review of user parameter-free robust adaptive beamforming algorithms," *Digital Signal Process.*, vol. 19, no. 4, pp. 567–582, Jul. 2009.
[9] S. Boyd and L. Vandenberghe, *Convex Optimization*. Cambridge, U.K.: Cambridge Univ. Press, 2004.